Rapid Communication

Organ distribution of severe acute respiratory syndrome (SARS) associated coronavirus (SARS-CoV) in SARS patients: implications for pathogenesis and virus transmission pathways

Yanqing Ding,[1]* Li He,[1] Qingling Zhang,[1] Zhongxi Huang,[1] Xiaoyan Che,[2] Jinlin Hou,[3] Huijun Wang,[1] Hong Shen,[1] Liwen Qiu,[3] Zhuguo Li,[1] Jian Geng,[1] Junjie Cai,[1] Huixia Han,[1] Xin Li,[1] Wei Kang,[1] Desheng Weng,[1] Ping Liang[1] and Shibo Jiang[4]*

[1]*Department of Pathology, Nan Fang Hospital, First Military Medical University, Guangzhou, China*
[2]*Department of Infectious Diseases, Nan Fang Hospital, First Military Medical University, Guangzhou, China*
[3]*Centre Laboratory, Zhujiang Hospital, First Military Medical University, Guangzhou, China*
[4]*Laboratory of Viral Immunology, Lindsley F. Kimball Research Institute, New York Blood Center, New York, USA*

*Correspondence to:
Shibo Jiang, Laboratory of Viral Immunology, Lindsley F. Kimball Research Institute, New York Blood Center, 310 East 67th Street, New York, NY 10021, USA.
E-mail: sjiang@nybloodcenter.org

and to:

Yanqing Ding, Department of Pathology, First Military Medical University, Guangzhou 5101515, China.
E-mail: dyq@fimmu.com

Abstract

We previously identified the major pathological changes in the respiratory and immune systems of patients who died of severe acute respiratory syndrome (SARS) but gained little information on the organ distribution of SARS-associated coronavirus (SARS-CoV). In the present study, we used a murine monoclonal antibody specific for SARS-CoV nucleoprotein, and probes specific for a SARS-CoV RNA polymerase gene fragment, for immunohistochemistry and *in situ* hybridization, respectively, to detect SARS-CoV systematically in tissues from patients who died of SARS. SARS-CoV was found in lung, trachea/bronchus, stomach, small intestine, distal convoluted renal tubule, sweat gland, parathyroid, pituitary, pancreas, adrenal gland, liver and cerebrum, but was not detected in oesophagus, spleen, lymph node, bone marrow, heart, aorta, cerebellum, thyroid, testis, ovary, uterus or muscle. These results suggest that, in addition to the respiratory system, the gastrointestinal tract and other organs with detectable SARS-CoV may also be targets of SARS-CoV infection. The pathological changes in these organs may be caused directly by the cytopathic effect mediated by local replication of the SARS-CoV; or indirectly as a result of systemic responses to respiratory failure or the harmful immune response induced by viral infection. In addition to viral spread through a respiratory route, SARS-CoV in the intestinal tract, kidney and sweat glands may be excreted via faeces, urine and sweat, thereby leading to virus transmission. This study provides important information for understanding the pathogenesis of SARS-CoV infection and sheds light on possible virus transmission pathways. This data will be useful for designing new strategies for prevention and treatment of SARS.

Copyright © 2004 Pathological Society of Great Britain and Ireland. Published by John Wiley & Sons, Ltd.

Introduction

The global outbreak of severe acute respiratory syndrome (SARS) in 2003 resulted in more than 8000 cases and 774 deaths [1]. It has been demonstrated that SARS-associated coronavirus (SARS-CoV) is the primary causative pathogen of SARS [2–6] and may originate from some wild animals, such as Himalayan palm civets [7]. Farzan's group has shown that angiotensin-converting enzyme 2 (ACE2) is a functional receptor for SARS-CoV [8]. The ACE2 binding site is located in the S1 domain of SARS-CoV spike (S) protein [9–11]. Jiang and colleagues have demonstrated that the heptad repeat 1 and 2 regions

in the S2 domain of S protein associate to form a fusion-active oligomeric core structure and a peptide derived from the HR2 region inhibits SARS-CoV infection [12].

The entire genome of SARS-CoV has been sequenced and it encodes RNA polymerase, spike (S) glycoprotein, membrane (M) glycoprotein, envelope (E) glycoprotein and nucleocapsid (N) protein [2–6,13]. The N protein in most coronaviruses is highly conserved, immunogenic and abundantly expressed during infection [14]. Therefore, it has been widely used as an important viral antigen in immunological and immunohistochemical assays for clinical diagnosis and laboratory detection of coronavirus infection.

It has been confirmed that SARS epidemics in 2003 started in the Guangdong Province of China [15]. Recently, new SARS cases have been identified in this region [16]. As medical research scientists working in this endemic area, we were the first systematically to analyse the autopsy tissues from patients who died of SARS in Nan Fang Hospital, Guangzhou, Guangdong and identified the major pathological changes [17]. However, we obtained limited data on the organ and tissue distribution of the SARS-CoV. Little information about the pathogenesis of this disease is available. This has significantly impeded the progress for designing more effective strategies for the prevention and treatment of SARS.

In the present study, we used immunohistochemistry and *in situ* hybridization to detect SARS-CoV in tissues from patients who died of SARS and gained insights into the pathogenesis and potential new transmission routes of SARS-CoV.

Materials and methods

Materials

Autopsy samples of lung, lymph node, spleen, heart, liver, kidney, adrenal gland, parathyroid gland, pituitary, bone marrow, skin, oesophagus, gastric fundus, small intestine, pancreas, thyroid, aorta, cerebrum, cerebellum, testis, ovary, uterus and striated muscle were obtained from four patients who died of SARS and four control patients who died of other diseases without SARS-CoV infection in the Eighth People's Hospital of Guangzhou City, the Second Affiliated Hospital of Zhongshan University, and the Guangzhou Institute of Respiratory Diseases, with documented permissions from patients' family members and the Health Administration of Guangdong Province, China. The ethical issues related to this study were reviewed and approved by the Research Administration Committees of the First Military Medical University and the local hospitals.

All four patients (three males aged 25, 38 and 57 years, and one 62-year-old female) met the diagnostic criteria for SARS defined by WHO [15]. All the patients were treated with ribavirin (an antiviral drug), and levofloxacin and doxycycline (antibacterial drugs). Only one was treated with steroids. The detailed clinical data and pathological findings have been reported previously [17,18]. These four SARS patients died on days 9, 10, 20 and 34, respectively, after onset of the disease. The four control patients were two males (32 and 52 years old) who suddenly died of dissecting aneurysm of the thoracic aorta and coronary heart disease, respectively, and two females (28 and 68 years old) who died as a result of ectopic pregnancy and cerebral haemorrhage, respectively.

Immunohistochemistry (IHC)

IHC was performed as described by Lin *et al* [14] using a mouse monoclonal antibody (mAb) directed against a recombinant SARS-CoV N protein [19]. Briefly, the autopsy tissue samples were fixed in 4% neutral formaldehyde, embedded in paraffin wax, sectioned at 4 μm, and incubated with 3% hydrogen peroxide to quench endogenous peroxidase activity. Microwave heat-induced antigen retrieval in citrate buffer (pH 6.0) was required for optimal staining [20]. Slides were incubated with the anti-N mAb (culture supernatants at 1 : 20 dilution) in a humid chamber at 4 °C overnight. After rinsing in PBS, the sections were incubated with goat anti-mouse IgG labelled with horseradish peroxidase (HRP) (DAKO, Carpinteria, CA) at 37 °C for 60 min. The slides were washed with PBS and counterstained with haematoxylin for 30 s. Antibody binding to the cells in tissues was detected with the HRP reaction kit (DAKO). The sections were then dehydrated, mounted with the Permount kit (Fisher Scientific, Pittsburgh, PA) and examined under a light microscope. SARS-CoV infected and uninfected Vero E6 cells were used as positive and negative controls, respectively.

Reverse-transcriptase polymerase chain reaction (RT-PCR)

RT-PCR for detection of the SARS-CoV M protein gene and RNA polymerase gene fragments was established in our laboratories as previously described [21]. Briefly, RNA was isolated from lung tissue using TRI-ZOL reagents (Invitrogen, Gaithersburg, MD) following the manufacturer's instructions. After this procedure, RNA was dissolved in 40 μl RNase-free water. RT-PCR was performed with the SuperScript One-Step RT-PCR kit (Invitrogen) and SARS-CoV gene-specific primers [3], ie, BNIoutS: 5′-ATG AAT TAC CAA GTC AAT GGT TAC-3′ and BNIoutAS: 5′-CAT AAC CAG TCG GTA CAG CTA C-3′ (RNA polymerase gene fragment of the SARS-CoV strain BJ01, nt 18 134–18 323, 190 bp), and MS2: 5′-ATG GCA GAC AAC GGT ACT ATT AC-3′ and MA2: 5′-CTT ACT GTA CTA GCA AAG C-3′ (M protein gene of the SARS-CoV strain BJ01, nt 26 379–27 045, 667 bp). RNA (1 μl) was subjected to RT-PCR in the GeneAmp PCR System 9700 (Applied Biosystems, Framingham, MA). Initial cycling was performed at 45 °C for 30 min, and 95 °C for 3 min, followed by 10 cycles at 94 °C for 15 s, 65–56 °C (drop 1 °C every cycle) for 15 s, and 72 °C for 35 s. The subsequent 30 cycles were performed at 94 °C for 15 s, 56 °C for 15 s, and 72 °C for 35 s.

In situ hybridization (ISH)

Sense and antisense digoxigenin-labelled SARS-CoV RNA polymerase gene-specific oligonucleotides (described above) were prepared through 3′ end-labelling reactions with kits from Boehringer Mannheim (Indianapolis, IN). ISH was performed on paraffin wax-embedded tissues with the ready-for-use reagents purchased from Boster Biological Technology Co

Ltd (Wuhan, China) following the manufacturer's instructions. Briefly, tissue sections were dewaxed in xylol and rehydrated with gradient ethanol. Endogenous peroxidase was quenched in 3% H_2O_2. The tissues were digested with 3 mg/ml pepsin in 0.14 mol/L citric acid at 37 °C for 20 min and incubated at 37 °C for 3 h with prehybridization buffer containing 50% deionized formamide, 5× standard saline citrate, 2% blocking reagent, 0.1% *N*-lauroylsarcosine, 0.02% sodium dodecyl sulphate and 100 ng/ml salmon sperm DNA. The tissue sections were hybridized with digoxigenin-labelled oligonucleotide probes (5 µg/ml) at 37 °C for 18 h. The slides were rinsed in a series of graded salt solutions (2×, 0.5× and 0.2× standard saline citrate). After reaction with a digoxigenin-labelled blocking reagent at 37 °C for 30 min, the sections were exposed to biotin-labelled mouse anti-digoxin antibody at 37 °C for 60 min, and incubated in avidin–peroxidase at 37 °C for 20 min. The peroxidase conjugates were subsequently localized by using the substrate diaminobenzidine tetrahydrochloride (DAB) and counterstained with Mayer's haematoxylin.

Pathological examination and histochemical staining

Specimens were fixed with 4% neutral formaldehyde and embedded in paraffin wax. Sections (4 µm) were stained with haematoxylin and eosin (H&E) and with Macchiavello stain, and examined under a light microscope.

Transmission electron microscopy

Specimens (about 2 mm × 2 mm × 2 mm) were obtained from the autopsy tissues and fixed with 2.5% glutaraldehyde in phosphoric buffer (pH 7.4), post-fixed with 1% osmate, dehydrated with gradient alcohol, embedded in Epon 812, double-stained with uranium acetate and lead citromalic acid, and observed under a JEM1200 transmission electron microscope (Jeol, Tokyo, Japan).

Results

The mouse mAb against SARS-CoV N protein was generated using a recombinant SARS-CoV (strain BJ01) N protein as immunogen as previously described [19]. In an enzyme-linked immunosorbent assay (ELISA), this mAb specifically recognized the recombinant SARS-CoV N protein with high binding affinity ($K_d = 4 \times 10^{-9}$ M), and reacted with convalescent sera from SARS patients, but was negative to the sera of healthy blood donors [22]. Using an immunofluorescence assay, we demonstrated that this mAb bound significantly to Vero E6 cells infected by SARS-CoV, but did not bind to uninfected Vero E6 cells, adenovirus-infected 293 cells or rotavirus-infected MA104 cells (Figure 1). The results suggest that this mAb is specific for the SARS-CoV N protein and can be used in IHC for detection of the distribution of SARS-CoV in organs and tissues from SARS patients.

Primers specific for the SARS-CoV RNA polymerase gene fragment BNI109 (SARS-CoV strain
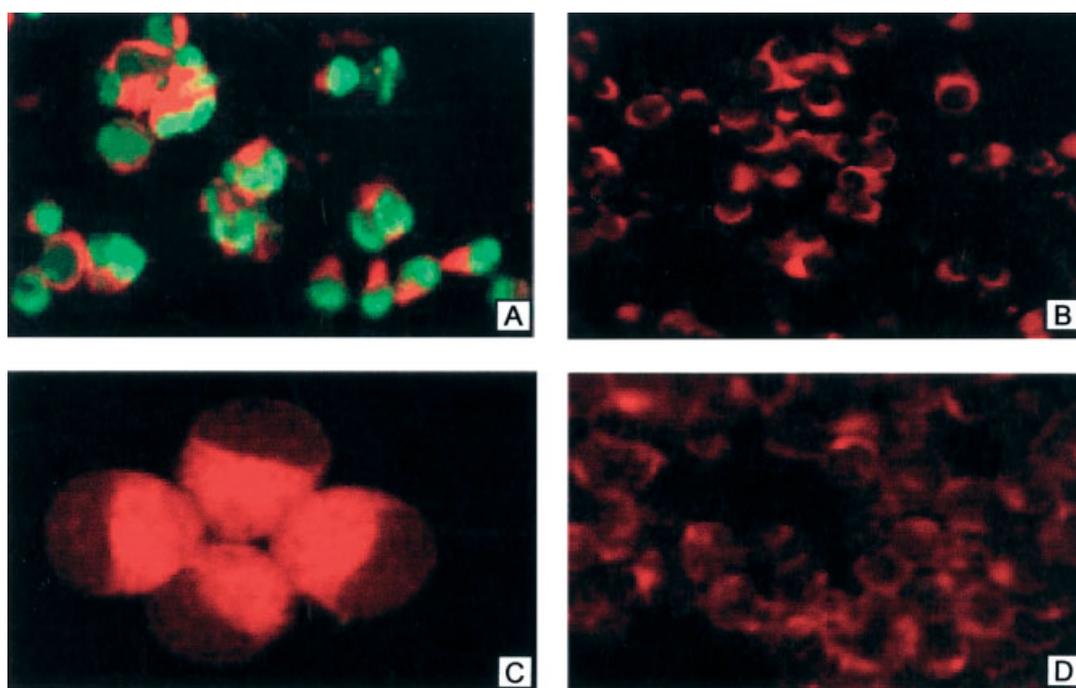
Figure 1. Detection of SARS-CoV N protein by immunofluorescence. (A) Vero E6 cells infected by SARS-CoV (×200). (B) Uninfected Vero E6 (×200); (C) 293 cells infected with adenovirus type 5 (×400). (D) MA104 cells infected by Group A rotavirus (×200). The green colour represents the positive signal for SARS-CoV N protein, while the negative cells without SARS-CoV infection display a red colour

BJ01, nt 18134–18323) were developed in our laboratories as previously described [21]. Using these primers to amplify the gene fragments from eight specimens (sputum samples, throat swabs and plasma) of established SARS cases by RT-PCR, all the resulting gene fragments possessed 100% identity to the sequence of the corresponding RNA polymerase gene fragments of SARS-CoV strain BJ01, confirming the specificity of these primers. The specificity of *in situ* hybridization was verified by disappearance or decrease of the signal after: (i) digestion of the sections with RNase A (0.2 mg/ml) (Sigma Chemical Co, St Louis, MO) for 2 h at 37 °C before ISH, and (ii) competition by adding an excess of unlabelled oligonucleotide probes. These preliminary results suggested that this ISH assay can be used for the detection of SARS-CoV in the organs and tissues of SARS patients.

To confirm further the specificity of the IHC and ISH assays described above, we first tested the lung tissues of four patients who died of SARS and four patients who died of other diseases using these two assays in parallel for detection of SARS-CoV N protein and RNA polymerase gene fragment, respectively. Our previous studies demonstrated that SARS-CoV can be detected in certain cell types, eg pneumocytes, in the lung tissues of SARS patients using different methods, including H&E and Macchiavello's stains for

observing inclusion bodies, and transmission electron microscopy for revealing corona-like virus particles [17,18]. In the present study, inclusion bodies and corona-like virus particles were observed in the lung tissues from all of the SARS patients (Figure 2A–C). However, no inclusion bodies or virus particles were identified in the lung tissues of the four control patients. The presence of SARS-CoV in the lung tissues of SARS patients was further confirmed by RT-PCR, since the SARS-CoV RNA polymerase gene fragment and M protein gene were identified in lung tissues from three SARS patients (Figure 2D; samples from the fourth patient were tested later and showed similar results, not included in this figure). However, these SARS-CoV RNA species were not found in lung tissues from the four control patients. These results confirm the observations by other groups that the respiratory system is the primary target for SARS-CoV [2–5].

Since the presence of SARS-CoV in lung tissues from these SARS patients was confirmed by the techniques described above, we used the IHC and ISH techniques to detect the SARS-CoV N protein and RNA polymerase gene fragment, respectively, in these lung tissues. Pneumocytes in the lung tissues of SARS patients, but not those from the four control patients, contained detectable SARS-CoV antigen and RNA. Two representative slides showing pneumocytes
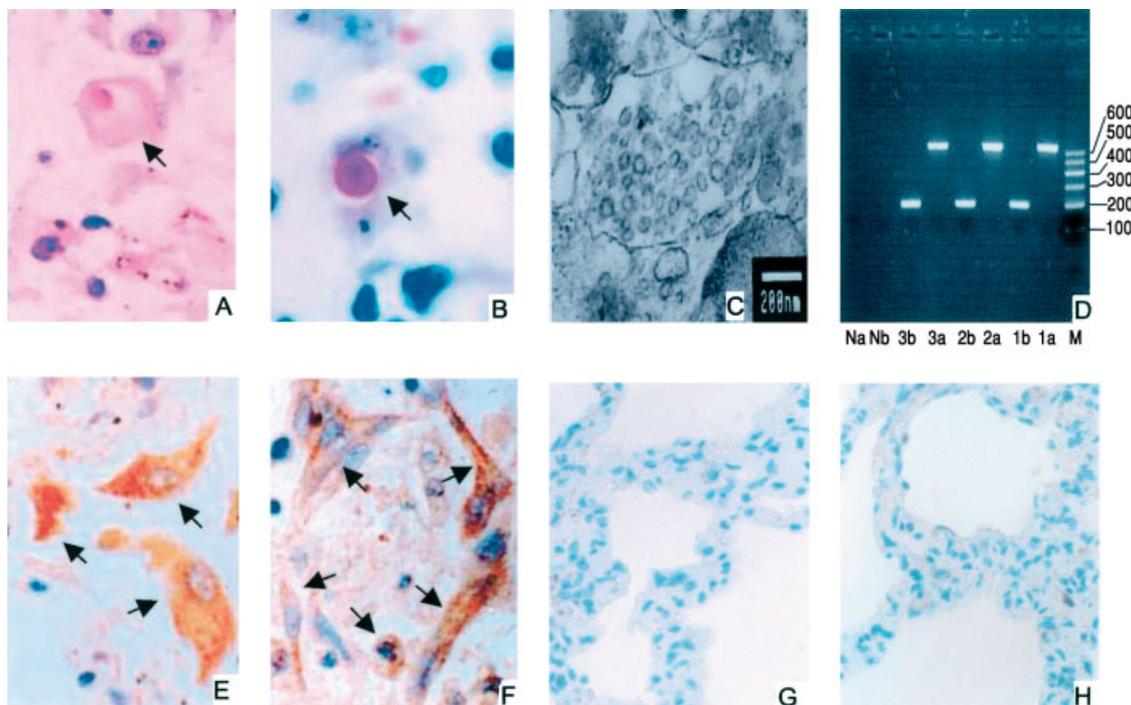
Figure 2. Detection of SARS-CoV in lung tissues from patients who died of SARS (A–F) and from a patient who died through rupture of a thoracic aortic aneurysm (G and H). (A) Viral inclusion body in a pneumocyte (arrow; H&E, ×400). (B) Viral inclusion body in a pneumocyte (arrow; Macchiavello's stain, ×400). (C) Clusters of corona-like viral particles in the endoplasmic reticulum of a type II alveolar epithelial cell (transmission electron microscopy; bar = 200 nm); (D) SARS-CoV M protein gene (a, 667bp) and RNA polymerase gene fragment (b, 190bp) detected in lung tissues from three SARS cases (1–3), but not in the negative control (N), who died through rupture of a thoracic aortic aneurysm (RT-PCR). M = marker. (E) SARS-CoV N protein expression in pneumocytes (IHC, ×400). (F) SARS-CoV RNA polymerase gene expression in pneumocytes (ISH, ×400); the positive cells (brown-yellow) are indicated by arrows. (G) SARS-CoV N protein expression (IHC, ×200). (H) SARS-CoV RNA polymerase gene expression (ISH, ×200) is not detectable in lung tissue from the individual who died through rupture of a thoracic aortic aneurysm

positive with the mAb specific for SARS-CoV N protein and with the probes specific for SARS-CoV RNA polymerase gene fragment are shown in Figure 2E and F, respectively. In contrast, none of the cells in the lung tissues of the four control patients were positive in both assays (Figure 2G and H). These results suggest that both IHC and ISH developed in our laboratories are specific and sensitive for the detection of SARS-CoV in organs and tissues.

Using these two validated assays, we examined other organs and tissues from the patients who died of SARS and the controls. If positive cells were observed, the number of positive cells and the total number of cells in 10 high-power views were counted under a microscope and scored as described in the footnotes to Table 1. As shown in Figure 3, SARS-CoV antigen and RNA were found in tracheal/bronchial serous gland epithelium, gastric parietal cells, small intestinal epithelium, acidophilic cells in parathyroid and pituitary, pancreatic acinar cells, adrenal cortical and medullary cells, sweat gland cells, epithelial cells of distal convoluted renal tubules, cerebral neurones and hepatocytes near the central vein (Table 1, Figure 3 1–11A and B). However, SARS-CoV N protein and RNA polymerase gene fragments were not detectable in heart (Figure 3 12A and B), seminiferous tubule of testis (Figure 3 13A and B), thyroid, oesophagus, spleen, lymph node, bone marrow, ovary, uterus, aorta, cerebellum and muscle (Table 1); and in corresponding tissues of control patients, namely glandular epithelium of the gastric corpus, mucosal and glandular small intestinal epithelia, pancreatic acini, bronchial mucous glandular epithelia, cerebral cortex, pituitary, liver, adrenal gland and cutaneous sweat glands (Figure 3 1–11C and D).

Discussion

There has been a warning that SARS epidemics may recur in future [23]; significantly, new SARS cases have recently been reported in Singapore [24] and China [16]. Therefore, the development of effective strategies for the protection of at-risk populations is urgently needed. However, the pathogenesis of SARS-CoV infection and the virus transmission pathways have not been clearly defined. The distribution of SARS-CoV in organs and tissues in SARS patients has not been systematically determined due to the lack of antibodies and probes specific for SARS-CoV. Recently, we developed an IHC assay, using a murine mAb specific for the SARS-CoV N protein, and an ISH method, using probes specific for the SARS-CoV RNA polymerase gene fragment, for *in situ* detection of SARS-CoV in tissues.

Consistent with our previous observations [17,25], SARS-CoV was predominantly detected in lung, trachea and bronchus. Strikingly, SARS-CoV was also detected in many other organs and tissues, including stomach, small intestine, distal convoluted renal tubule, sweat gland, parathyroid, pituitary, pancreas, adrenal, liver and cerebrum (Figure 3 and Table 1).

Table 1. Detection of SARS-CoV in tissues from four SARS autopsies[a]

Organs and tissues	A1061[b]		A1062[b]		A1065[b]		A1076[b]	
	IHC	ISH	IHC	ISH	IHC	ISH	IHC	ISH
Lung	+++	+++	+++	+++	+++	+++	+++	+++
Stomach	++	++	+	+	+	+	+	+
Small intestine	++	++	+	+	+	+	+	+
Kidney	++	++	++	++	++	++	++	++
Adrenal	++	++	++	++	++	++	++	++
Skin	++	++	++	++	++	++	++	++
Parathyroid	++	++	++	++	++	++	++	++
Pituitary	+	+	+	+	+	+	+	+
Liver	+	+	+	+	+	+	+	+
Cerebrum	+	+	+	+	+	+	+	+
Pancreas	+	+	+	+	+	+	−	−
Oesophagus	−	−	−	−	−	−	−	−
Bone marrow	−	−	−	−	−	−	−	−
Thyroid	−	−	−	−	−	−	−	−
Spleen	−	−	−	−	−	−	−	−
Lymph node	−	−	−	−	−	−	−	−
Cerebellum	−	−	−	−	−	−	−	−
Heart	−	−	−	−	−	−	−	−
Striated muscle	−	−	−	−	−	−	−	−
Testis	−	−	−	−	−	−	−	−
Ovary	−	−	−	−	−	−	−	−
Uterus	−	−	−	−	−	−	−	−

[a] The number of positive cells and the total number of cells specified were counted in 10 high-power views. The percentage of positive cells was calculated. 0%, 1 to <24%, ≥25% to <49%, ≥50% to <74%, and ≥75% positive cells were recorded as '−', '+', '++', '+++', and '++++', respectively. No positive signal was detected in control tissues.
[b] Case number.
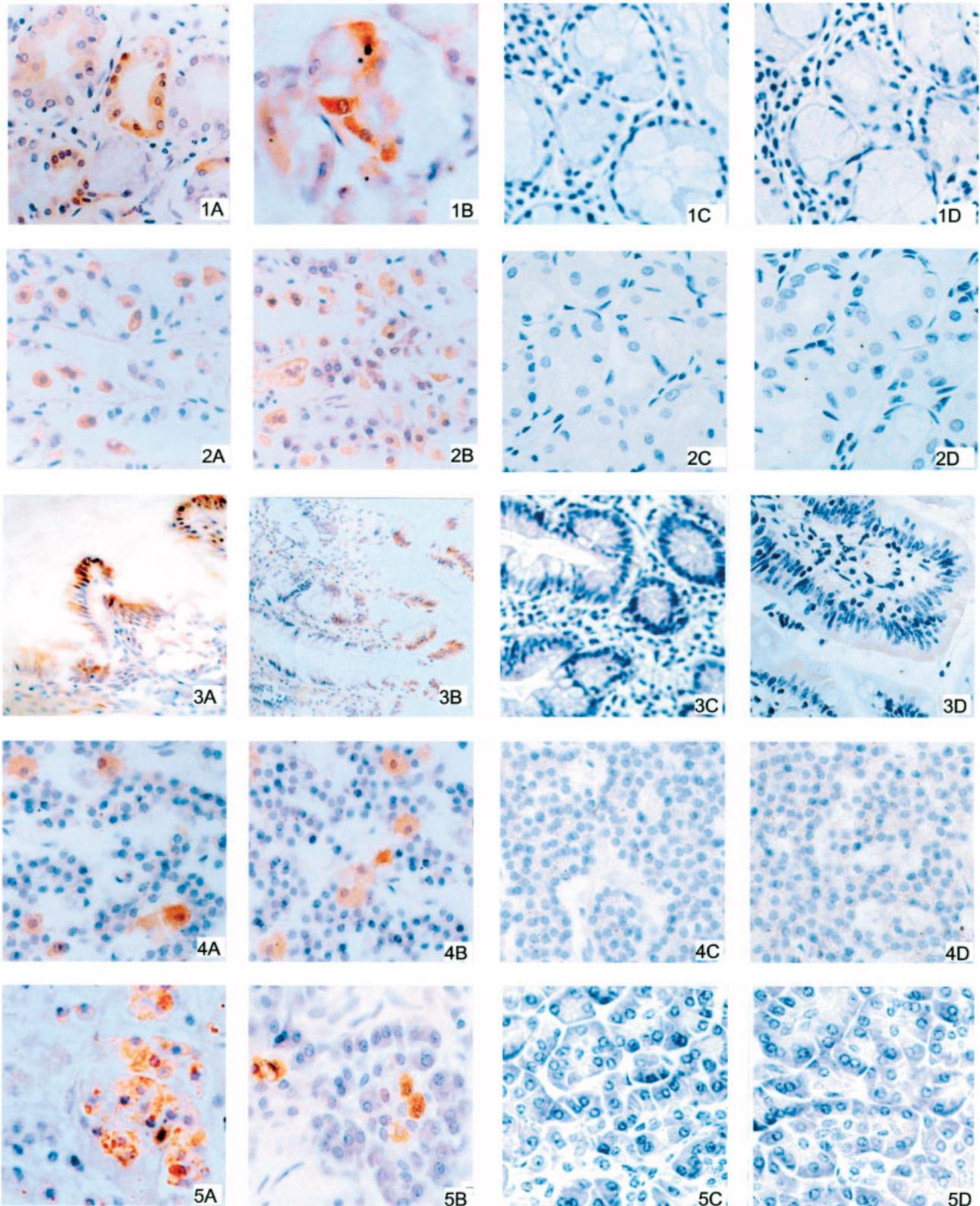
Figure 3. Detection of SARS-CoV N protein by IHC (A and C) and of SARS-CoV RNA polymerase gene fragments by ISH (B and D) in the following samples from SARS patients (A and B; DAB; figures 3, 7A, 8A, 10, 13 ×200; figures 1, 2, 4–6, 8B, 9, 11, 12 ×400; 7B ×480) and from control patients (C and D; DAB; figures 1–11 ×400). (1) Bronchial serous gland epithelium; (2) gastric parietal cells; (3) small intestinal epithelium; (4) acidophilic cells of parathyroid; (5) pancreatic acinar cells; (6) acidophilic cells of pituitary; (7) adrenal cortical cells; (8) sweat gland cells; (9) cerebral neurones; (10) epithelial cells of distal convoluted renal tubule; (11) hepatocytes near the central vein; (12) myocardium; (13) seminiferous tubules of testis. The brownish-yellow colour in cells represents positive signal for SARS-CoV N protein in IHC, and for SARS-CoV RNA polymerase gene fragments in ISH
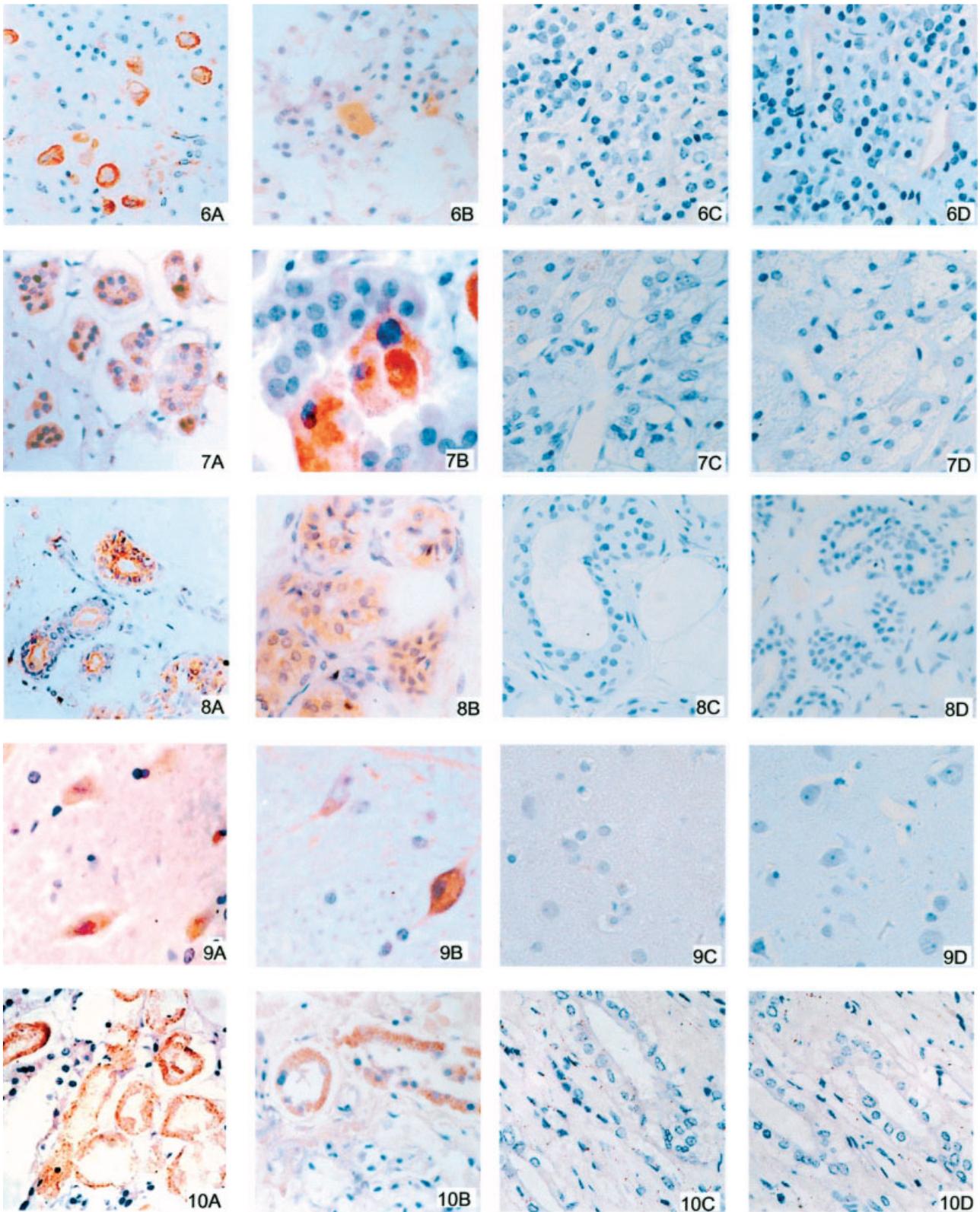
Figure 3. Continued
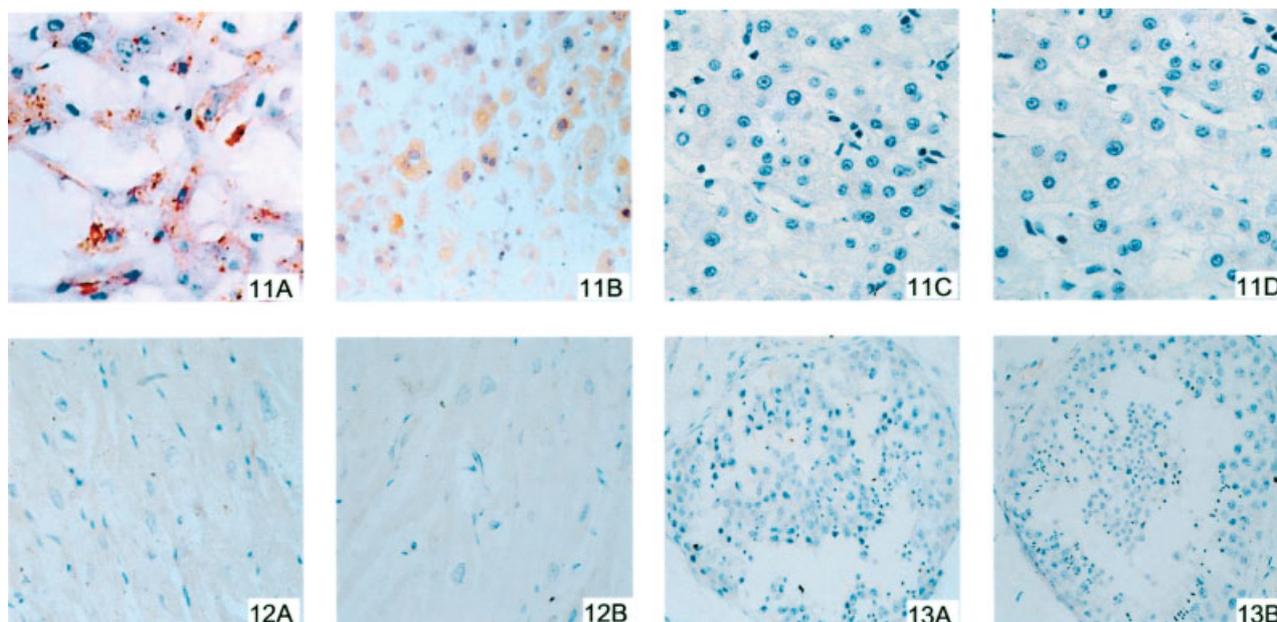
Figure 3. Continued

However, the virus was not detected in oesophagus, thyroid, spleen, lymph node, bone marrow, testis, ovary, uterus, heart, aorta, cerebellum or muscle (Table 1). These results suggest that, in addition to the respiratory system, the gastrointestinal system may also be a primary target of SARS-CoV, ie virus in contaminated food and water may enter the human body through epithelial cells covering the surface of the gastrointestinal tract, although there is no direct evidence to show that food-borne SARS-CoV is transmitted through the gastrointestinal system. Other organs with detectable SARS-CoV may be secondary targets of SARS-CoV, ie the virions in blood that are released from the primary target (eg respiratory system) may infect cells in these organs and tissues. Another possibility is that SARS-CoV may not infect these cells, but rather binds specifically or non-specifically to their surface, resulting in detection of SARS-CoV antigens and RNA. The pathological changes in these organs and tissues may be caused directly by the cytopathic effect (CPE) mediated by SARS-CoV replication in these organs; or indirectly by the systemic toxic reaction due to failure of the respiratory system, or by the harmful immune response and cytokine reaction induced by virus infection.

Aminopeptidase N (CD13) is a receptor for at least two human coronaviruses [26,27] and was proposed as a receptor for SARS-CoV [28]. It was recently demonstrated that ACE2 is a functional receptor for SARS-CoV [8] and a fragment in the S1 domain of the SARS-CoV S protein is responsible for binding of the virus to ACE2 [9–11]. Analyzing 72 human tissues by real-time PCR, Harmer et al [29] demonstrated that ACE2 is expressed in human lung, gastrointestinal tract, kidney, heart and testis. Consistent with our results, SARS-CoV was detected in lung, gastrointestinal tract and kidney, suggesting that

SARS-CoV may utilize ACE2 as a receptor to enter the cells in these organs. However, it is unclear why the cells in heart and testis cannot be infected by SARS-CoV despite the expression of high levels of ACE2.

Consistent with the report of Leung et al, who used electron microscopic and histological examination of endoscopic biopsies and post mortem material [30], we also detected SARS-CoV in the epithelial cells of the alimentary tract, including stomach and small intestine (Table 1). This suggests that the gastrointestinal system may also be an entry route for SARS-CoV present in food or water. Although there is no report of such transmission [15], caution should be exercised by the at-risk population during the SARS-CoV endemic season. This finding supports the hypothesis that SARS-CoV may be released into the environment via faeces from individuals infected by SARS-CoV. Indeed, low levels of SARS-CoV RNA were detected in faeces from SARS patients [3,30]. Moreover, we also found SARS-CoV in the epithelial cells of the distal convoluted renal tubule, suggesting that SARS-CoV may also be transmitted through contaminated urine.

For the first time, we have demonstrated that SARS-CoV is detectable in sweat gland cells in the skin. This suggests another route of transmission for SARS-CoV, since this virus may be excreted in sweat and infect other people who are in direct contact with the patient's skin. Indeed, Rados suspected that SARS-CoV could be transmitted by direct touch [31]. If this transmission route is confirmed, new infection-control measures should be recommended. For example, patients may have to wear gloves, disposable gowns and eye protection, in addition to N95 masks, and to avoid kissing or touching other people.

References

1. WHO. Summary of probable SARS cases with onset of illness from 1 November 2002 to 31 July 2003. www.who.int [2003].

2. Ksiazek TG, Erdman D, Goldsmith CS, *et al*. A novel coronavirus associated with severe acute respiratory syndrome. *N Engl J Med* 2003; **348**: 1953–1966.

3. Drosten C, Gunther S, Preiser W, *et al*. Identification of a novel coronavirus in patients with severe acute respiratory syndrome. *N Engl J Med* 2003; **348**: 1967–1976.

4. Peiris JS, Lai ST, Poon LL, *et al*. Coronavirus as a possible cause of severe acute respiratory syndrome. *Lancet* 2003; **361**: 1319–1325.

5. Marra MA, Jones SJM, Astell CR, *et al*. The genome sequence of the SARS-associated coronavirus. *Science* 2003; **300**: 1399–1404.

6. Rota PA, Oberste MS, Monroe SS, *et al*. Characterization of a novel coronavirus associated with severe acute respiratory syndrome. *Science* 2003; **300**: 1394–1399.

7. Guan Y, Zheng BJ, He YQ, *et al*. Isolation and characterization of viruses related to the SARS coronavirus from animals in Southern China. *Science* 2003; **302**: 276–278.

8. Li WH, Moore MJ, Vasilieva NY, *et al*. Angiotensin-converting enzyme 2 is a functional receptor for the SARS coronavirus. *Nature* 2003; **426**: 450–454.

9. Wong SK, Li W, Moore MJ, *et al*. A 193-amino-acid fragment of the SARS coronavirus S protein efficiently binds angiotensin-converting enzyme 2. *J Biol Chem* 2003; **279**: 3197–3201.

10. Xiao X, Chakraborti S, Dimitrov AS, *et al*. The SARS-CoV S glycoprotein: expression and functional characterization. *Biochem Biophys Res Commun* 2003; **312**: 1159–1164.

11. Dimitrov DS. The secret life of ACE2 as a receptor for the SARS virus. *Cell* 2003; **115**: 652–653.

12. Liu S, Xiao G, Chen Y, *et al*. Interaction between the heptad repeat 1 and 2 regions in spike protein of SARS-associated coronavirus: implication for virus fusogenic mechanism and identification of fusion inhibitors. *Lancet* 2004; **363**: 938–947.

13. Kuiken T, Fouchier RAM, Schutten M, *et al*. Newly discovered coronavirus as the primary cause of severe acute respiratory syndrome. *Lancet* 2003; **362**: 263–270.

14. Lin Y, Shen X, Yang RF, *et al*. Identification of an epitope of SARS-coronavirus nucleocapsid protein. *Cell Res* 2003; **13**: 141–145.

15. WHO. Consensus document on the epidemiology of severe acute respiratory syndrome (SARS). www.who.int 2003.

16. Macfie, N. China confirms SARS case in Southern Guangzhou. Reuters Health Information. www.medscape.com/viewarticle /466 710 2004.

17. Ding Y, Wang H, Shen H, *et al*. The clinical pathology of severe acute respiratory syndrome (SARS): a report from China. *J Pathol* 2003; **200**: 282–289.

18. Wang H, Ding Y, Li X, *et al*. Fatal aspergillosis in a patient with SARS who was treated with corticosteroids. *N Engl J Med* 2003; **349**: 507–508.

19. Che XY, Qiu LW, Pan YX, *et al*. Rapid and efficient preparation of monoclonal antibodies against SARS-associated coronavirus nucleocapsid protein by immunizing mice. *Di Yi Jun Yi Da Xue Xue Bao* 2003; **23**: 640–642.

20. Lounsbury KM, Stern M, Taatjes D, *et al*. Increased localization and substrate activation of protein kinase C delta in lung epithelial cells following exposure to asbestos. *Am J Pathol* 2002; **160**: 1991–2000.

21. Yang J, Wang ZH, Chen JJ, *et al*. Clinical detection of polymerase gene of SARS-associated coronavirus. *Di Yi Jun Yi Da Xue Xue Bao* 2003; **23**: 424–427.

22. Che XY, Hao W, Qiu LW, *et al*. Antibody response of patients with severe acute respiratory syndrome (SARS) to nucleocapsid antigen of SARS-associated coronavirus. *Di Yi Jun Yi Da Xue Xue Bao* 2003; **23**: 637–639.

23. Enserink M. SARS in China. The big question now: will it be back? *Science* 2003; **301**: 299.

24. Enserink M. Infectious diseases: Singapore lab faulted in SARS case. *Science* 2003; **301**: 1824.

25. Ding Y, Wang HJ, Shen H, *et al*. Study on etiology and pathology of severe acute respiratory syndrome. *Zhonghua Bing Li Xue Za Zhi* 2003; **32**: 195–200.

26. Yeager CL, Ashmun RA, Williams RK, *et al*. Human aminopeptidase N is a receptor for human coronavirus 229E. *Nature* 1992; **357**: 420–422.

27. Delmas B, Gelfi J, L'Haridon R, *et al*. Aminopeptidase N is a major receptor for the entero-pathogenic coronavirus TGEV. *Nature* 1992; **357**: 417–420.

28. Kontoyiannis DP, Pasqualini R, Arap W. Aminopeptidase N inhibitors and SARS. *Lancet* 2003; **361**: 1558.

29. Harmer D, Gilbert M, Borman R, *et al*. Quantitative mRNA expression profiling of ACE 2, a novel homologue of angiotensin converting enzyme. *FEBS Lett* 2002; **532**: 107–110.

30. Leung WK, To KF, Chan PK, *et al*. Enteric involvement of severe acute respiratory syndrome-associated coronavirus infection. *Gastroenterology* 2003; **125**: 1011–1017.

31. Rados C. SARS: protecting against a deadly disease. *FDA Consum* 2003; **37**: 14–17.